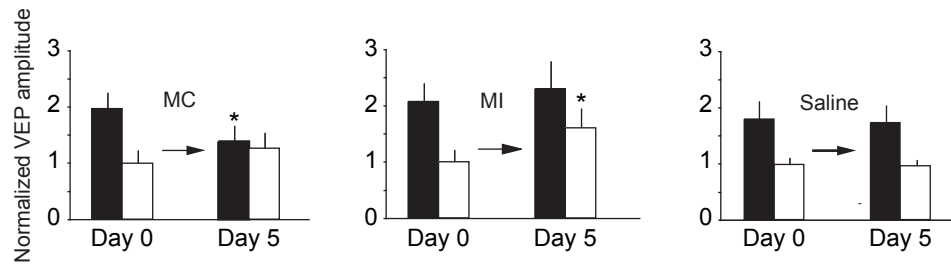


Thalamic activity that drives visual cortical plasticity

Monica L. Linden, Arnold J. Heynen,
Robert H. Haslinger and Mark F. Bear

Supplementary Materials

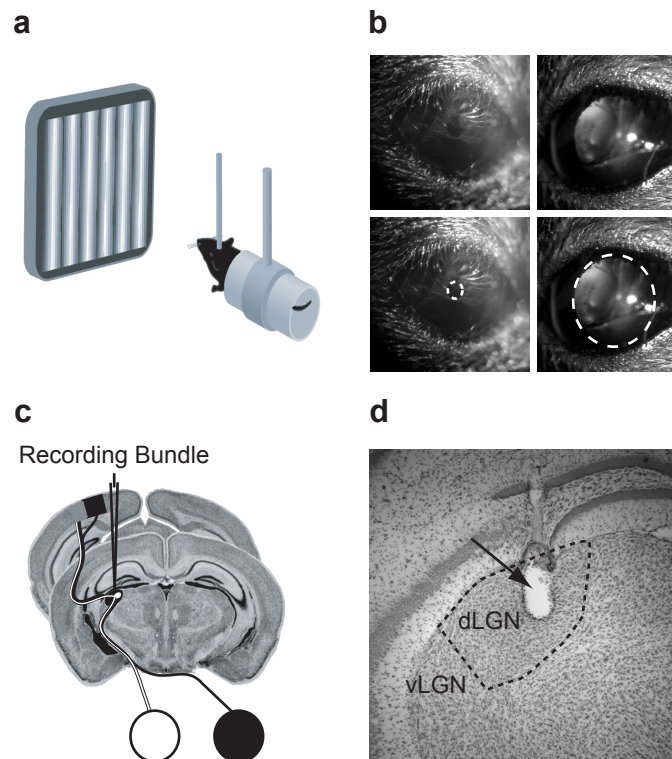
Figure S1



Monocular eyelid closure (MC) and monocular retinal inactivation (MI) lead to ocular dominance shifts by distinct mechanisms (adapted from Frenkel and Bear, 2004).

Visually evoked potentials (VEPs) were obtained from the primary visual cortex of juvenile mice as they viewed sinusoidal gratings through the eye contralateral (black bar) or ipsilateral (white bar) to the recording electrode. Recordings were made before (Day 0) and after 5 days of eye manipulation (Day 5) with all manipulations performed on the contralateral eye. Data are normalized to the baseline (day 0) ipsilateral VEP amplitude. Baseline values show approximately a 2:1 ratio of contralateral to ipsilateral (C/I) VEP amplitude. Following 5 days of MC, there is a statistically significant decrease in the deprived (contralateral) eye VEP amplitude (left panel), resulting in a C/I ratio nearer to 1:1. A shift in the C/I ratio is also observed after MI, but this is due to an increase in the non-deprived (ipsilateral) eye response, with no change in the inactivated (contralateral) eye response (center panel). Five days of saline injection into the contralateral eye, without manipulating experience, has no effect on the VEP response (right panel).

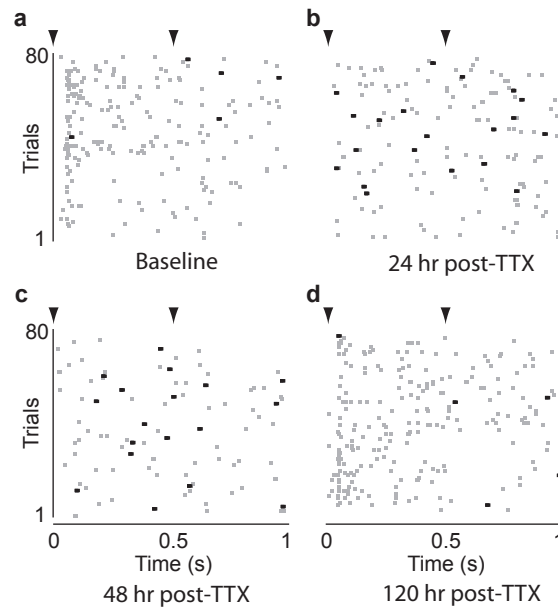
Figure S2



Methodology.

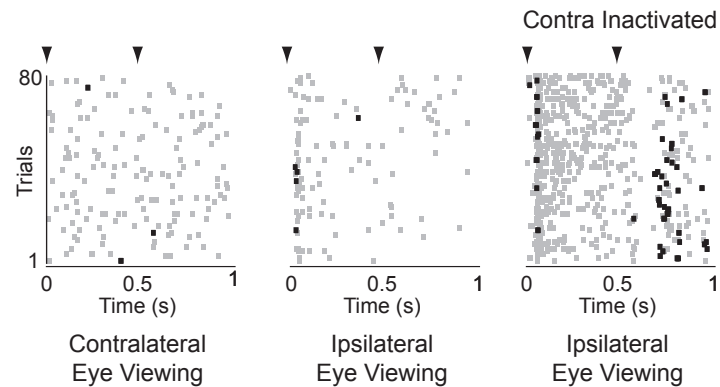
a, Experimental setup. Data were obtained from awake, head-restrained mice viewing grating stimuli or movies of natural visual stimuli. **b**, Intraocular delivery of tetrodotoxin (TTX) was confirmed by pupillary dilation. Left column: non-injected eye, right column: TTX-injected eye. Lower row: circles outline the pupil. **c**, Schematic of recording electrode placement in the dLGN. **d**, Histological confirmation of recording electrode track in dorsal LGN. Arrow indicates site of electrolytic lesion ($10 \mu\text{A}$; 10 s) made at the end of recording session.

Figure S3



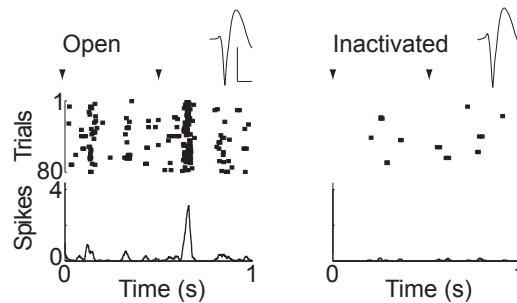
An increase in the percentage of spikes in bursts persists throughout an extended period of monocular inactivation.

a-d, Raster plots of dLGN activity during 80 stimulus trials recorded at different times following an intraocular TTX injection in a chronically implanted mouse. Conventions as for Fig 2. Black squares represent spikes in bursts; gray squares non-burst spikes. **a**, baseline condition 2 hrs prior to TTX injection; **b -c**, 24 and 48 hrs after TTX injection, respectively; **d**, recovery from TTX, 120 hrs after injection. Note that the neurons are visually responsive only during the baseline and recovery conditions (**a**, **d**), and the marked increase in bursts throughout the period of inactivation (**b - c**). Panel **c** is same as in **Fig 2c**.

Figure S4

Inactivation of the contralateral eye changes the firing patterns of the dLGN ipsilateral core.

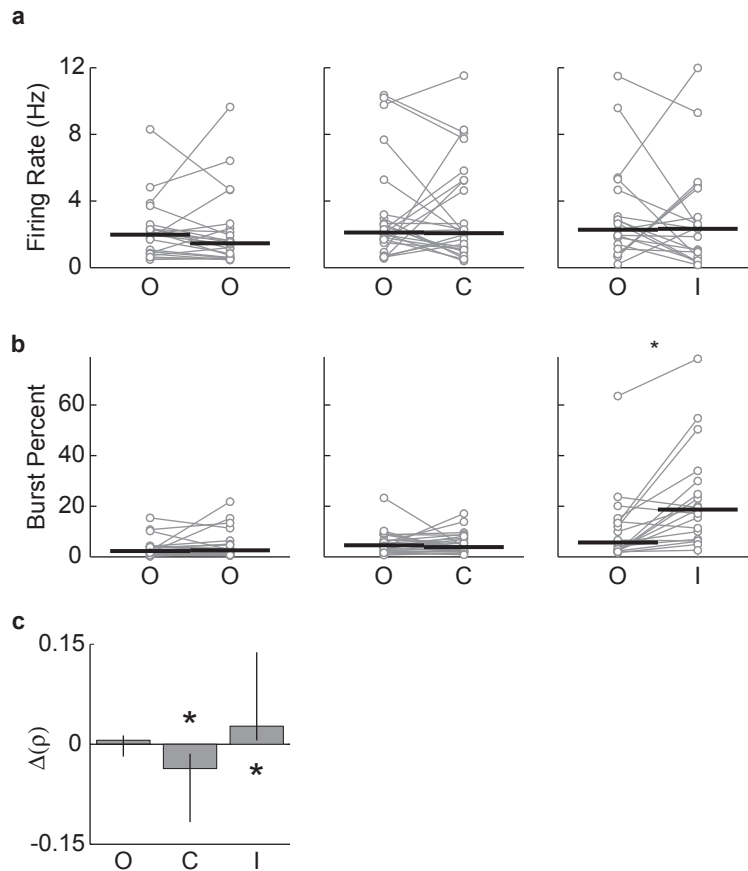
Raster plots of 80 stimulus trials from a representative dLGN neuron responsive to the ipsilateral eye. Black squares represent spikes in bursts; gray squares non-burst spikes. Note bursts on the leading edge of the visual response when the ipsilateral (center panel) but not contralateral (left panel) eye is viewing. Following inactivation of the contralateral eye (right panel), the visual response to the ipsilateral eye is maintained, but additionally shows a marked increase in bursts and overall firing. See also **Fig 2e-f**.

Figure S5

Monocular retinal inactivation decreases dLGN firing rate if the animal is under Nembutal anesthesia.

Peristimulus time histograms and raster plots (80 stimulus trials) for one representative neuron are presented. Stimuli were presented at 90° , 1 Hz phase reversing at the arrows. Spike waveforms are averages over the entire recording session. Scale bar: 100 μ V, 500 μ s. Left panel: responses during baseline; right panel: after MI. Note that burst spikes are much more prevalent under barbiturate anesthesia during the baseline period than in the awake mouse preparation (see **Fig 2a,b**).

Figure S6



The effects of monocular eyelid closure (MC) and monocular retinal inactivation (MI) on dLGN activity when assessed using natural scene stimuli.

All animals also viewed natural scene movies (excerpts from *Microcosmos: Le peuple de l'herbe*, presented in grayscale, consisting of one 30s segment shown 10 times and one 4 minute segment shown twice) between presentations of the sinusoidal gratings, with all stimuli presented in a pseudorandom fashion. Analyses were performed as described in the Supplementary Methods. **a**, Monocular eyelid closure (C) and monocular retinal inactivation (I) have no effect on dLGN firing rate ($p > 0.7$, KW). Connected circles represent the same neuron recorded before and after eye manipulation. Black lines indicate the median values (control: $n = 22$ neurons (9 animals), $p > 0.3$ WSR; MC: $n = 24$ neurons (12 animals), $p > 0.8$; MI: $n = 19$ neurons (8 animals), $p > 0.5$). **b**, MI increases the percentage of spikes in bursts ($p < 0.01$ KW; control: $n = 22$ neurons (9 animals), $p > 0.8$; MC: $n = 24$ neurons (12 animals), $p > 0.8$; MI: $n = 19$ neurons (8 animals), $p < 0.01$ WSR). **c**, MC leads to a decrease in spike correlation ($p < 10^{-4}$, KW; MC: $n = 20$ neuron pairs (6 animals), $p < 10^{-3}$ WSR). Bars represent the median change in area under the cross-correlogram following visual manipulation. Error bars show the interquartile range (control: $n = 22$ neuron pairs (6 animals), $p > 0.9$; MI: $n = 18$ neuron pairs (6 animals), $p < 0.02$).

Supplementary Discussion

How monocular eyelid closure triggers deprived-eye depression

It has been known for decades that the change in dLGN activity during monocular eyelid closure causes rapid depression of deprived-eye responses in the visual cortex. Theoretically, this could occur as a consequence of either a *decrease* or a *de-correlation* of deprived-eye input to cortex relative to the seeing eye¹. This distinction is important for understanding cortical plasticity. The former explanation suggests a mechanism whereby active inputs “punish” inactive inputs (heterosynaptic depression); the latter explanation requires a mechanism by which the activity of poorly correlated inputs triggers their own demise (homosynaptic depression). Our data reveal no difference in the amount or temporal structure of dLGN activity following monocular eyelid closure. Instead, our findings support the “homosynaptic” hypothesis that poorly correlated dLGN activity is the trigger for deprived-eye depression in visual cortex².

One methodological concern is that the apparent decrease in correlative firing during monocular eyelid closure stems from the choice of visual stimuli in the “normal visual experience” condition. Because the animals viewed a full-screen sinusoidal grating, there may have been an artificial increase in simultaneous firing during baseline viewing, as neurons with non-overlapping receptive fields may be activated together. To address this concern, the animals were also shown “natural scene” images, in the hopes of better approximating the types of visual input the animal would be exposed to during a period of monocular eyelid closure that leads to an ocular dominance shift. The maintenance of overall dLGN firing activity under all viewing conditions, the increase in burst spikes during monocular retinal inactivation, and the decrease in correlated firing during monocular eyelid closure all hold when the animal is viewing the natural scene stimuli (**Fig S6**). Thus, a robust distinction between “normal visual experience” and monocular eyelid closure is the degree of correlation of dLGN neurons.

It is of interest to consider these findings in the context of the influential BCM theory of visual cortical plasticity³. According to the BCM modification algorithm, synaptic depression occurs whenever presynaptic input activity (termed **d** by BCM) arrives at the same time that integrated postsynaptic cellular responses (**c**) are below a modification threshold (θ); the value of θ is set dynamically by a running average of the

postsynaptic cell's activity. The level of postsynaptic response at any moment ($c(t)$) depends crucially on how correlated the presynaptic activity is of converging LGN inputs (as well as on the strength of these synapses). Well-correlated LGN activity evokes a large integrated postsynaptic response; poorly correlated LGN activity evokes a weak integrated postsynaptic response. During monocular eyelid closure, the inputs from the non-deprived eye continue to evoke strong responses in visual cortex, which holds the value of θ at a high level. Consequently, the weak responses evoked in response to the poorly correlated input from the deprived eye consistently fall below θ , and these synapses undergo homosynaptic depression. The rate of depression increases with the amount of deprived-eye input activity as long as this is poorly correlated¹.

Unlike monocular eyelid closure, brief binocular eyelid closure has little effect on responses in visual cortex⁴. How does the BCM theory account for this finding? Because the poorly correlated inputs from both eyes fail to evoke strong responses in visual cortex, the value of θ falls to a low level. Therefore, even though the inputs from the two eyes are poorly correlated and are incapable of evoking strong responses, the integrated postsynaptic responses that do occur hover around the (lowered) value of θ . Consequently, there is little synaptic depression during binocular deprivation.

How monocular retinal inactivation protects inputs from synaptic depression

Based on measurements in anesthetized animals⁵⁻⁷ (see **Fig 2g-h**), it was hypothesized that dLGN inputs during monocular retinal inactivation are protected from the effects of monocular eyelid closure because they are silenced, and therefore not conveying the de-correlated afferent activity that triggers a loss of synaptic strength^{4,5,8}. In addition, it has been hypothesized that increases in cortical responsiveness following monocular retinal inactivation are a consequence of homeostatic adjustments of synaptic weights in the face of reduced thalamic input^{9,10}. Our results suggest that these hypotheses might need to be revisited since they are based on false assumptions about the effects of monocular retinal inactivation on dLGN activity.

The current findings provide a surprising alternate explanation for the lack of deprived-eye depression following monocular retinal inactivation. The active, patterned firing of dLGN neurons during monocular retinal inactivation may protect against

deprived-eye depression, in essence, by substituting for normal visual experience. That is, from the point of view of a postsynaptic cortical neuron, well-correlated input activity caused by synchronous LGN bursting satisfies the conditions required to maintain synaptic strength (as does “normal visual experience”). Our findings continue to support the idea that monocular retinal inactivation abolishes the poorly correlated “noise” that triggers LTD in visual cortex during monocular eyelid closure, but by an entirely different mechanism than was assumed previously.

The increase in responsiveness to the non-deprived eye after monocular retinal inactivation is thought to reflect a homeostatic response to lowered cortical activity^{4,11}. A goal for future studies is to analyze the effects of viewing condition on activity in visual cortex, and to correlate these with changes in dLGN activity. However, it is already clear from the data obtained in this study that any reduction in cortical activity during monocular retinal inactivation is not accounted for by silencing thalamic input. Indeed, the surprising finding of a substantial increase in the activity of the dLGN postsynaptic to the non-deprived eye (**Fig 2e-f**) suggests an alternative explanation for open-eye response potentiation. Instead of (or in addition to) the synaptic potentiation being a consequence of postsynaptic AMPA receptor scaling¹¹ or metaplasticity⁴, it could be a reflection of Hebbian plasticity driven by an increase in stimulus-evoked presynaptic activity.

How can we account for the remarkable transformations of dLGN activity after monocular retinal inactivation? Bursting activity in dLGN during monocular retinal inactivation resembles that observed during sleep. In this state, the reduction in non-retinal inputs from the brainstem and cortex cause dLGN neurons to hyperpolarize, leading to de-inactivation of T-type Ca^{2+} channels that generate periodic bursts in response to other inputs that depolarize the neurons beyond threshold¹². In the awake animal, inactivating tonic input from the retina appears to put the dLGN neurons into a similar firing mode. The work of Weliky and Katz¹³ suggests that corticothalamic inputs may trigger burst firing. At this point, we can only speculate about how inactivation of the contralateral retina causes such a robust change in dLGN activity postsynaptic to the ipsilateral eye. Possible mechanisms include changes in the activity of local dLGN circuitry, intrathalamic circuitry via the thalamic reticular nucleus, or corticothalamic feedback. More work is required to distinguish among these possibilities.

1. Blais, B. S., Shouval, H. Z. & Cooper, L. N. in *Proc Natl Acad Sci U S A* 1083-7 (1999).
2. Rittenhouse, C. D. et al. Stimulus for rapid ocular dominance plasticity in visual cortex. *J Neurophysiol* **95**, 2947-50 (2006).
3. Bienenstock, E. L., Cooper, L. N. & Munro, P. W. Theory for the development of neuron selectivity: orientation specificity and binocular interaction in visual cortex. *J Neurosci* **2**, 32-48 (1982).
4. Frenkel, M. Y. & Bear, M. F. How monocular deprivation shifts ocular dominance in visual cortex of young mice. *Neuron* **44**, 917-923 (2004).
5. Rittenhouse, C. D., Shouval, H. Z., Paradiso, M. A. & Bear, M. F. Monocular deprivation induces homosynaptic long-term depression in visual cortex. *Nature* **397**, 347-50 (1999).
6. Stryker, M. P. & Harris, W. A. Binocular impulse blockade prevents the formation of ocular dominance columns in cat visual cortex. *J Neurosci* **6**, 2117-33 (1986).
7. Kaplan, E., Purpura, K. & Shapley, R. M. Contrast affects the transmission of visual information through the mammalian lateral geniculate nucleus. *J Physiol* **391**, 267-88 (1987).
8. Heynen, A. J. et al. Molecular mechanism for loss of visual cortical responsiveness following brief monocular deprivation. *Nat Neurosci* **6**, 854-62 (2003).
9. Desai, N. S., Cudmore, R. H., Nelson, S. B. & Turrigiano, G. G. Critical periods for experience-dependent synaptic scaling in visual cortex. *Nat Neurosci* **5**, 783-9 (2002).
10. Maffei, A. & Turrigiano, G. G. Multiple modes of network homeostasis in visual cortical layer 2/3. *J Neurosci* **28**, 4377-84 (2008).
11. Mrsic-Flogel, T. D. et al. Homeostatic regulation of eye-specific responses in visual cortex during ocular dominance plasticity. *Neuron* **54**, 961-72 (2007).
12. Sherman, S. M. Tonic and burst firing: dual modes of thalamocortical relay. *Trends Neurosci* **24**, 122-6 (2001).
13. Weliky, M. & Katz, L. C. Correlational structure of spontaneous neuronal activity in the developing lateral geniculate nucleus in vivo. *Science* **285**, 599-604 (1999).

Supplementary Methods

Subjects

Juvenile, male C57/BL6 mice (Charles River Laboratories) were group housed, on a 12 hr/12 hr light/dark cycle, with food and water available *ad libitum*. All animals were treated according to NIH and MIT guidelines for animal use.

Surgical preparation for acute in vivo recording

P25 Animals were anesthetized with 50 mg/kg ketamine and 10 mg/kg xylazine (i.p.). Using cyanoacrylate, a fixation post was attached to the skull anterior to bregma. The skull above the dLGN (2.0 mm posterior to bregma, 2.0 mm lateral to the midline) was demarcated for future acute recording and the skull surrounding the location was encircled by a plastic ring affixed with cyanoacrylate. An EEG electrode was placed in occipital cortex, and a reference electrode was placed in frontal cortex. Electrodes were secured with cyanoacrylate and dental cement was used to cover the entire skull exposure outside of the plastic ring.

Following surgery animals were monitored for signs of infection or discomfort. Habituation to the restraint apparatus began ≥ 24 hours post-recovery. Animals remained in the restraint system for ≥ 3 habituation sessions lasting ≥ 30 minutes each prior to the acute recording session.

Acute recording

Animals were placed in the restraint apparatus and anesthetized with Isoflurane (1.5-3.0% in 100% oxygen). A craniotomy was performed over the dLGN of one hemisphere. Isoflurane was discontinued and the animal was allowed to recover from anesthesia while remaining in the restraint system. A recording bundle consisting of seven microwires was lowered into the dLGN. Visually-driven unit activity was used to aid in the placement of the bundle. In all cases, placement of the electrodes in the dLGN was confirmed histologically (see **Fig S2**). Single unit activity and simultaneous EEG activity were recorded using “Recorder” software (Plexon, Inc., Dallas, TX). Single units were discriminated offline using “Offline Sorter” (Plexon, Inc.). In experiments where

the animals were anesthetized throughout the recording session (see Fig. S4), Nembutal was administered (100 mg/kg s.c.).

Stimulus delivery

The visual stimuli were generated using custom MATLAB software (The Mathworks, Natick, MA) and the Psychophysics Toolbox function set (psychtoolbox.org). The video monitor, suitably linearized by γ -correction, was positioned 16 cm from the subjects' eyes and centered on the midline, occupying $82.5^\circ \times 100^\circ$ of the visual field. Visual stimuli consisted of full-screen sinusoidal gratings (0.05 cycles/ $^\circ$, 100% contrast), alternating in phase (phase reversed) at a temporal frequency of 1, 2 and 4 Hz in both horizontal and vertical orientations. Stimuli were presented in a pseudorandom fashion.

Eyelid closure

Mice were anesthetized by inhalation of Isoflurane (1.5 – 3.0% in 100% oxygen). Eyelids were held closed with Vetbond tissue adhesive (3M, St. Paul, MN).

TTX injection

Mice were anesthetized by inhalation of Isoflurane (see above). A small puncture was made in the vitreous chamber using a 30-gauge needle. TTX (1 μ L, 1 mM, Sigma, St. Louis, MO) was then injected into the vitreous chamber using a microsyringe (10 μ l, Hamilton Co, Reno, NV). Following syringe withdrawal, the eye was rinsed with sterile eye drops. The efficacy of retinal blockade by TTX was confirmed by a tonic and fully dilated pupil (see **Fig S2**).

Comparison of pre- and post-manipulation firing rates and burst percentages

Three groups of neurons were recorded under baseline and post-manipulation conditions. To determine the statistical significance of any manipulation-induced firing rate or burst percentage changes, a two-step procedure was used. We first tested if the median firing rate change differed significantly between groups using a non-parametric Kruskal-Wallis (KW) test. Second, we tested if the median firing rate change for each of

the groups was significantly different from zero using non-parametric Wilcoxon Sign-Rank (WSR) tests. Non-parametric tests were used as the data were not normally distributed.

Comparison of pre- and post-manipulation ISI distributions

Mean ISI distributions for each group and condition were constructed using a bootstrapping method and compared using Kolmogorov-Smirnov (KS) tests. First, for each group, a neuron was randomly selected with replacement. Next, an ISI was randomly selected with replacement from the set of all ISIs recorded from that neuron. This procedure was repeated N times where N was the mean number of ISIs recorded from all neurons in the group. The resulting set of ISIs, a random sample of the group's mean ISI distribution, was subjected to a KS test. This procedure was repeated 1000 times, and the mean of the p-value recorded.

Comparison of pre- and post-manipulation pairwise correlation

To determine if correlated firing, beyond that predicted by chance, existed between pairs of neurons, the Bernoulli correlation coefficient

$$\rho(\delta) = \frac{P_{12}(\delta) - p_1 p_2}{\sqrt{p_1(1-p_1)p_2(1-p_2)}}$$

between the neurons' spike trains was calculated¹. $P_1(P_2)$ is the firing probability per bin of neuron 1 (2) and $P_{12}(\delta)$ the probability of joint firing at time lag δ . Positive (or negative) departures of ρ from zero indicate synchronous (or anti-synchronous) firing. To check the statistical significance of manipulation induced correlation changes, the change in ρ across each lag was calculated and summed over lags from -10 ms to 10 ms for each pair of neurons before and after manipulation. KW and WSR tests were then applied as above.

1. Aertsen, A.M., Gerstein, G.L., Habib, M.K. & Palm, G. Dynamics of neuronal firing correlation: modulation of "effective connectivity". *J Neurophysiol* **61**, 900-917 (1989).